

Suppression of Thermal Effect on Closed Loop Fiber Optic Gyroscope

A. Venkata Anuhya* and N. Venkatram

Department of Electronics and Computer Engineering, KL University, Guntur - 522 502, Andhra Pradesh, India; anuhya409@gmail.com, venkatram@kluniversity.in

Abstract

Fiber Optic Gyroscope (FOG), an inertial sensor measures the angular rotation of an object based on the principle of Sagnac effect. FOG is subjected to various environmental disturbances such as temperature, vibration etc., when it is operated in real time. Temperature variation is the major factor that affects the gyro performance. In this paper, a novel compensation approach called temperature soaking method has been presented which makes the gyro insensitive to temperature. This method has been carried out for a 3-axis (Gx, Gy and Gz) FOG and its outputs (bias values) were taken at different temperature points. In order to reduce the bias drift of FOG output, this method uses linear curve fitting function to generate the bias error coefficients. The generated bias error coefficients are subtracted from the existing bias data, which in turn reduces the bias error. The bias values obtained for 3-axis gyro at temperature points from -20°C to $+60^{\circ}\text{C}$ before compensation is then compared with the bias values obtained for after compensation at same temperature points. Experimental results demonstrate that, after compensation the bias drift greatly reduced from 15 to $0^{\circ}/\text{hr}$ approximately. This method effectively improves the stability and performance of a gyro and makes it to withstand to different environmental conditions which in turn increases the range of applications from military, navigation to space.

Keywords: Bias Error Coefficients, Compensation, Fibre Optic Gyroscope (FOG), Linear Curve Fitting Function, Thermal Drift, Temperature Soaking Method

1. Introduction

Earlier Inertial Navigation System (INS) which uses mechanical gyroscopes² was complex, limited dynamic range, bandwidth, reliability and takes large reaction time. Recent advances in development of optical gyroscopes such as Ring Laser Gyros (RLG) and Fibre Optics Gyros (FOG) became the conventional counterparts to mechanical gyros because of wide dynamic range, high accuracy, low reaction time and no 'g' sensitivity drift. However RLG technology is complex, because of large power requirements, size, weight and cost which in-turn limits its usage³. Optical communication and silicon technology are the two growing fields which support fibre optic gyro technology for the development of fibre optic gyroscope. Fibre optic sensors can be broadly classified based on sensing location, operating principle

and its applications^{4,5}. FOG is an extrinsic type phase modulated sensor consists of Integrated Optic Chip (IOC), temperature controlled Super Luminescent Diode (SLD) and Polarization Maintaining (PM)⁶ fibre along with digital signal processing electronics.

FOGs are mainly designed for the measurement of rotation induced path difference as a measure of frequency or phase difference between two counter propagating waves. FOG is described in two different configurations: Interferometric Fibre Optic Gyroscope (IFOG) and (RFOG) Resonant Fibre Optic Gyroscope. RFOG devices are similar to ring laser gyros whose performance is limited by the back scattering noise from the fibre⁷.

The signal processing scheme of a FOG is done in two ways: open loop and closed loop. Open loop configuration⁸ suffers with changes in amplitude and returning optical power variations of differential phase modulation

* Author for correspondence

which causes non-linearity behaviour and scale factor instability in the output of FOG⁹. To overcome these problems 'closed-loop configuration' is implemented. The open loop output is given as feedback to the input of phase modulator which nullifies the Sagnac phase shift error. CLFOG has multiple advantages over OLFOG i.e. output is independent of input light intensity variations, high accuracy, system gain, wide-dynamic range, high resolution, controlled phase bias, linearity, less reaction time and stability¹⁰.

1.1 Problem Definition

One major factor that affects the performance of gyro is thermal drift. The surrounding environment of FOG is often accompanied with the changes in temperature. The stability of the output of gyro, directly affects the accuracy of the inertial navigation system. Identifying the temperature effect among individual optical blocks is a complicated task, because of the non linearity's present in the optical blocks. Hence the compensation phenomenon for the complete gyro is done in the signal processing system. In order to reduce the random drift of FOG output, error compensation method is proposed to improve FOG's accuracy based on the temperature characteristics of gyro's output.

2. Literature Survey

Many researchers have been proposed their views about the design and implementation of closed loop fiber optic gyroscope and provide some error solving methods to achieve inertial grade performance. A concise review of recent researches is presented here.

Design of hardware circuit for the digital closed loop control system of FOG based on FPGA has been presented by Q. D. Sun, et al¹¹, and summarized the parameter demands for each module of closed loop control circuit. He proposed twice closed loop technique improved the zero offset stability of FOG. And, the digital signal processing by software in FPGA is also convenient for parameter adjustment in experiment. This technique greatly reduces the development period and improves the reliability of the system. Particularly, the author discussed the problems of component selection and the anti-jamming measures for PCB design to improve the performances of the system and also developed some samples of FOG using this

design method. The experiment shows that zero-biases of all samples are less than 0.075⁰/hr. But the fluctuations in the zero-biases of FOG during warm up and at extreme temperatures limit its application areas.

A method for compensating the Shupe effect errors caused by temperature in a fiber gyro was found out by Eberhard Handrich¹². A closed loop fiber optic gyro which includes a VCO control loop and an evaluation unit that incorporates a model which is dependent on the optical path The author's invention is based upon the fact that changes in optical path length $n*L$ (where n is the refractive index of the optical fiber and L is length of the fiber coil), causes asymmetries of the winding. The drift bias in the output signal of the fiber optic gyro is compensated on the basis of such model.

3. Design Approach of Closed-Loop Fiber Optic Gyroscope

The block diagram of digital phase ramp type closed loop fiber optic gyroscope is shown in Figure 1. CLFOG is modulated with square wave signal whose period is equal to the transit time (τ) of the fiber-coil. Square wave modulation is preferred for the modulation of light to increase the sensitivity and to detect the rotation rate polarity.

The PINFET (Photo Detector) converts optical power, which is output of FOG to electrical signal. The output of the detector is the square wave modulated co-sinusoidal signal. On-board ADC which is 16-bit parallel interface receives the data from PINFET through signal conditioning amplifier, process and digitize the data with a sampling frequency that must be equal to transit frequency of gyro i.e., 1 sample per transit time. This sampled data coming from ADC (16-bits) is demodulated synchronously, passing through a moving average filter to extract the phase error present in the detector output. The result is then multiplied with gain factor (received through UART). Dead band compensator is used to compensate the problem of dead zone and spikes in a signal if any. The integrator integrates the error signal with respect to transit time of the coil and generates the step size, used for the generation of feedback phase nullifying signal (staircase ramp). The amplitude of the ramp signal must be equal to the 2π voltage of the IOC (Integrated Optic Chip). Therefore, an integral controller is used with a

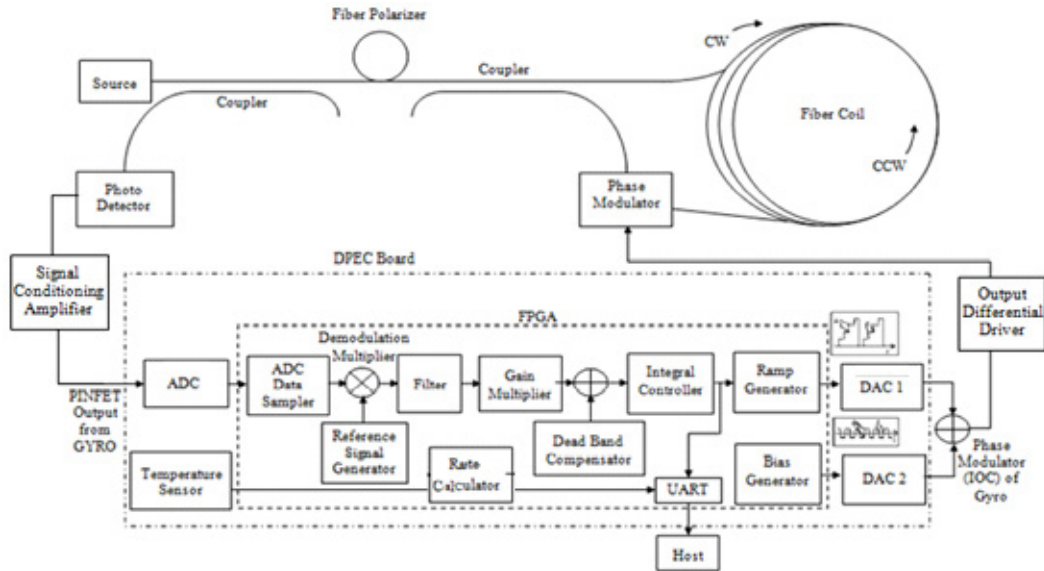


Figure 1. Design Approach of CLFOG.

variable gain to nullify the rotation induced Sagnac phase error of gyro. The output of the ramp generator is nothing but the phase-error-compensation signal. This technique is known as “digital serrodyne modulation technique”.

Digital Phase Estimator Card (DPEC) board acts as data acquisition and signal processing unit to achieve closed loop configuration of FOG. For every 2.5 ms, it transfers the integrator output and on-board temperature data to the PC for reducing the bias errors induced by the temperature, upon the request of synchronization pulses. Such fiber gyros are also called phase nulling gyros. One more advantage of digital configuration, compared to analog solution, is stability in phase during signal recovering. This type of gyros improves the accuracy to $0.001^\circ/\text{sec}$ to achieve inertial grade performance. But gyro performance is limited when it subjected to different environmental conditions. These problems can be reduced by using temperature compensation.

4. Proposed Method

FOG is affected with the changes in temperature. As the temperature varies, then it introduces the variations in the gyro parameters mainly the bias, leads to change in scale-factor, which will bring errors to the output of FOG.

4.1 Effects of Temperature Variations

The variation of environmental temperature will affect the refractive index of optical fibre induces the thermal

non-reciprocity effect, leading to cause sensor errors (i.e., Bias, Scale factor, linearity errors etc).

An effective compensation temperature soaking method is used to compensate the thermal drift of the sensor errors according to the temperature change rate during the operation. The process is dependent on the temperature provided by the internal temperature sensor of the IMU (Inertial Measurement Unit). Official thermal calibration requires professional equipment such as a thermal chamber, PC (Personal Computer) and a power supply. Such equipment can be used to get reliable thermal calibration results over a large temperature range.

4.2 Temperature Soaking Method

The Soak method works as follows: (1) Stabilize the temperature of the sensor at a certain temperature point; (2) Record the sensor measurements and calculate the sensor errors corresponding to such point; (3) Repeat this process at several typical temperature points, then the sensor errors along with temperature data can be obtained. By stabilizing the temperature, the Soaking method provides most reliable values of the sensor errors at the chosen temperature points.

4.3 Temperature Sensor Interfacing to FPGA

Signal processing has been carried out through Field Programmable Gate Array. FPGA reads the temperature data from sensor through I2C interface is shown in Figure 2. While reading temperature data, FPGA acts as master

I2C device and sensor as slave. On receiving a 2.5 msec from an external sync pulse, FPGA generates serial clock on SCL line and read data from bi-directional SDA line.

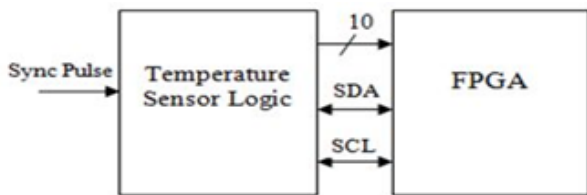


Figure 2. Temperature Sensor Interfacing To FPGA.

5. Working Principle

The aim of FOG temperature drift compensation is to make FOG output insensitive to the variation of temperature and its input-output characteristic are to be strictly linear (i.e., the nonlinearity error is very small) and bias should be very less. The setup for the compensation of FOG temperature drift is shown in Figure 3.

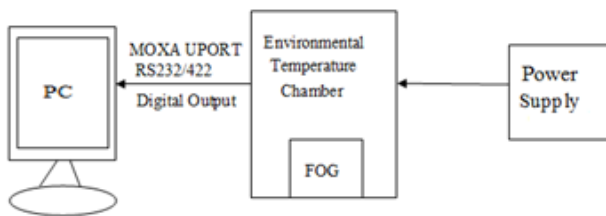


Figure 3. Test setup for proposed model.

A three axis gyro (i.e. Gx, Gy and Gz) is mounted in a stationary base and is kept horizontally in a temperature chamber.

- After giving the power supply, the data from the gyro is received for every 2.5ms synchronization pulse. A static test has been taken for some time to stabilize the temperature.
- Then power-on the chamber and set the chamber to -20°C. Capture the data for 1 to 2 hours until the temperature get stabilized at -20°C from room temperature.
- When the temperature gets stabilized, the corresponding gyro and temperature data were noted. Similarly the same process is repeated for various temperatures -10°C, 0°C, 10°C, 20°C, 30°C, 40°C, 50°C and 60°C. Repeatable test is performed to ensure that the same gyro data is maintained approximately at all times.
- After that, calculate the mean value of three cycles of raw data in counts of both temperature and 3-axis gyro. These mean values, can be used to generate the bias error coefficients by the rate calculator module.

- The rate calculator module, removes the temperature dependent bias variations present in the raw rate using the look up table (Bias error ROM) is shown in Figure 4. The on-board temperature sensor output value acts as an address for the compensation table. The output of the compensator block is the equivalent bias to be removed from the “raw rate” at that particular temperature.
- That means the coefficient value must be subtracted from the existing gyro data in order to reduce the bias drift of the gyro.

Again power-on the chamber and set the temperature to -20°C. Similarly the same process has to be repeated and observe the corresponding gyro’s and temperature data for -10°C, 0°C, 10°C, 20°C, 30°C, 40°C, 50°C and 60°C temperature change rates. The bias drift value can varies up to a maximum of 5⁰/hr. If the drift is greater than 5⁰/hr, indicates that the compensation is not done properly.

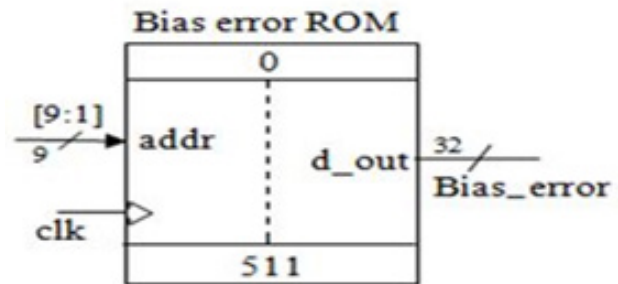


Figure 4. LUT Based Bias error ROM.

5.1 Generation of bias error coefficients

The error coefficients are generated with the help of MATLAB program. The program was written using linear curve fitting function that fits the curve linearly with its slope and intercept. The means values obtained are compared with the fitted curve and the program generates the error values which were present corresponding to each temperature point.

Example: The bias value for any particular temperature (say 30°C) is 120 counts. The output of the temperature sensor is 10 bit digital data representing 120 counts. Of the 10 bit data, 9 bits are used to calculate the address of the error value. Because one right shift of data makes the bias value to half i.e. 120/2 = 60. This value 60 represents the address location (of 512 locations) of the error coefficient present in the bias error ROM look up table. The overall process is done by rate calculator module. Then finally this error value is subtracted from the previous existing bias value which in turn reduces the error.

6. Results

6.1 OTR Results before Compensation

The 3 axis gyro and temperature data from -20°C to 60°C are for different cycles such as cycle 1, cycle 2 and cycle 3 are shown in Figures 5, 6 and 7:

Cycle 1.

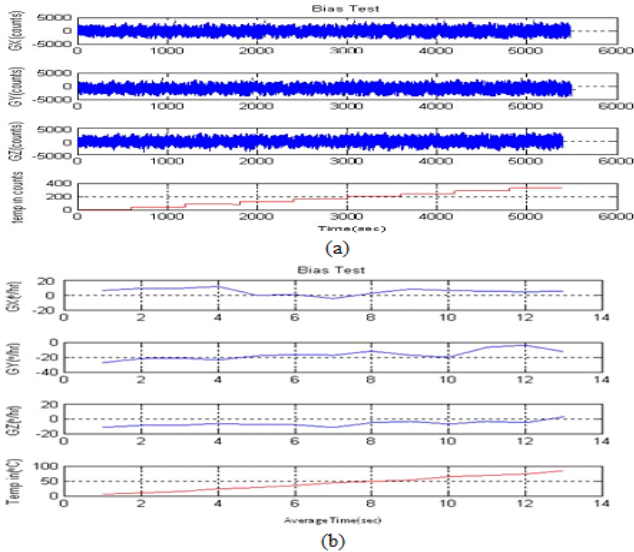


Figure 5. (a) Gx, Gy and Gz data from - 20°C to 60°C and (b) Averaged Gx, Gy and Gz data from - 20°C to 60°C for cycle 1.

Cycle 2.

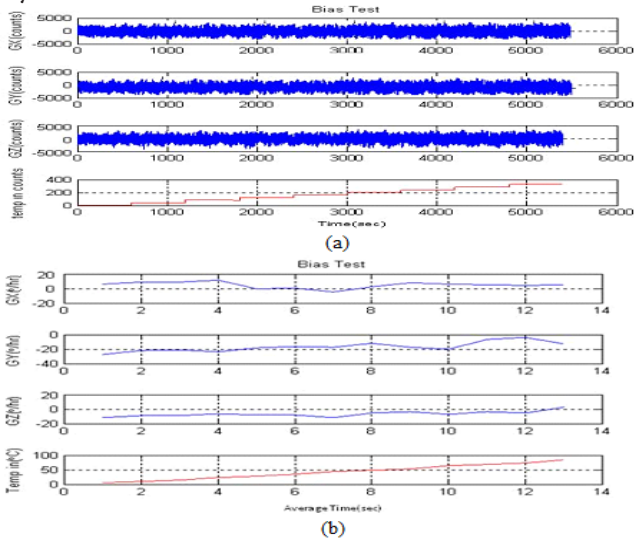


Figure 6. (a) Gx, Gy and Gz data from - 20°C to 60°C and (b) Averaged Gx, Gy and Gz data from - 20°C to 60°C for cycle 2.

Cycle 3.

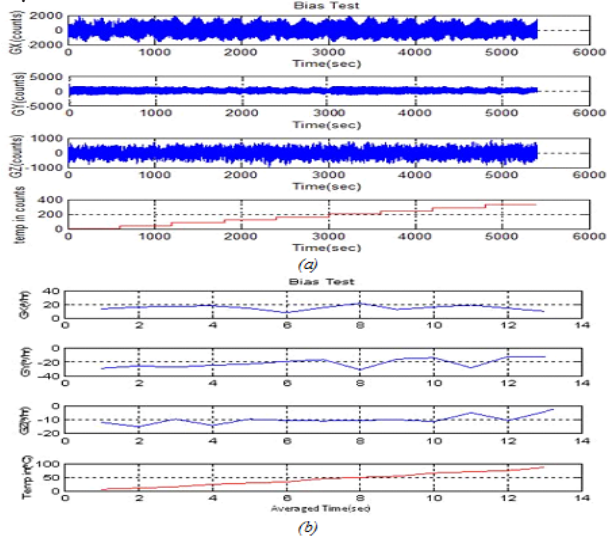


Figure 7. (a) Gx, Gy and Gz data from - 20°C to 60°C and (b) Averaged Gx, Gy and Gz data from - 20°C to 60°C for cycle 3.

The overall bias values in terms of counts and °/hr for each temperature of a three axis gyro for three cycles such as cycle 1, cycle 2 and cycle 3 are listed in Table 1.

6.2 OTR Results after Compensation

The raw and average data of 3-axis gyro from -20°C to 60°C after compensation as shown in Figure 8;

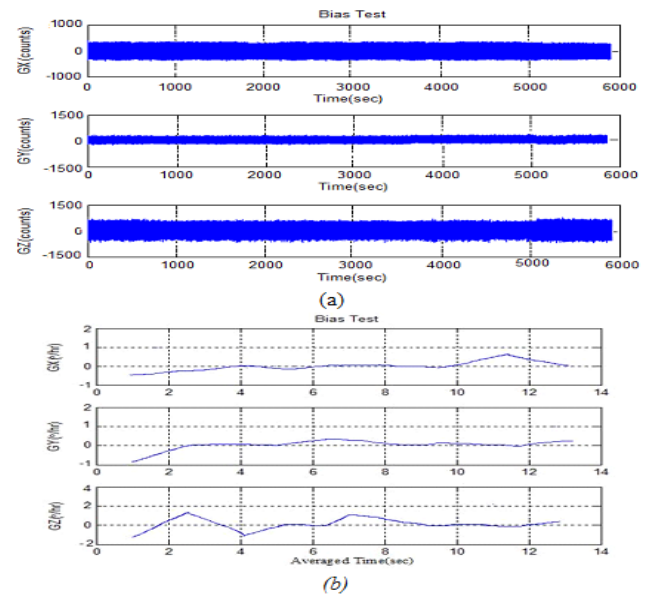


Figure 8. (a) Gx, Gy and Gz Raw data from - 20°C to 60°C and (b) Averaged Gx, Gy and Gz data from - 20°C to 60°C after compensation.

Table 1. (I) Cycle 1 (II) Cycle 2 (III) Cycle 3 OTR results before compensation

28V (mA)	TEMP	TEMP (COUNTS)			TEMP (°C)			BIAS (COUNTS)			BIAS (°/HR)		
		GX_	GY_	GZ_	GX_	GY_	GZ_	GX	GY	GZ	GX	GY	GZ
670	60	339.5727	342.9061	329.2314	84.9	85.7	82.3	11439.3100	-15698.4900	-892.5262	10.93	-12.87	-0.69
630	50	298.0527	300.2587	285.8692	74.5	75.1	71.5	13448.8800	-18008.5900	-10065.5700	12.86	-14.76	-7.84
600	40	256.9299	258.1617	244.0001	64.2	64.5	61.0	15838.9600	-19940.3500	-11477.8500	15.14	-16.34	-8.94
580	30	216.0733	216.9234	202.4436	54.0	54.2	50.6	17288.1400	-22007.6600	-12310.5700	16.53	-18.04	-9.59
580	20	176.8545	177.0991	162.6509	44.2	44.3	40.7	17534.0900	-24581.3800	-14099.0000	16.76	-20.15	-10.98
570	10	136.6474	136.4302	121.9552	34.2	34.1	30.5	17426.3100	-26859.7900	-13239.0400	16.66	-22.01	-10.31
570	0	97.3975	97.0756	81.8728	24.3	24.3	20.5	16332.9000	-29761.3500	-14446.1100	15.61	-24.39	-11.25
570	-10	58.5041	57.7064	43.2460	14.6	14.4	10.8	15755.2000	-31881.3200	-14772.1800	15.06	-26.13	-11.50
580	-20	18.8051	17.6126	3.2744	4.7	4.4	0.8	14772.9200	-33517.9900	-15183.3400	14.12	-27.47	-11.82

(I)

28V (mA)	TEMP	TEMP (COUNTS)			TEMP (°C)			BIAS (COUNTS)			BIAS (°/HR)		
		GX_	GY_	GZ_	GX_	GY_	GZ_	GX	GY	GZ	GX	GY	GZ
670	60	339.5381	342.9193	329.1490	84.9	85.7	82.3	10707.0200	-15227.5700	-1241.7410	10.23	-12.47	-0.96
630	50	297.9588	300.2317	285.8461	74.5	75.1	71.5	12837.1300	-17606.8700	-9529.7170	12.27	-14.42	-7.42
600	40	256.7448	258.0506	243.8409	64.2	64.5	61.0	15083.3500	-19415.4100	-10554.6300	14.41	-15.91	-8.21
580	30	215.9348	216.8723	202.3633	54.0	54.2	50.6	16337.9200	-21342.1200	-11601.6800	15.61	-17.49	-9.03
570	20	176.7003	177.1559	162.6213	44.2	44.3	40.7	16297.8300	-23899.2400	-13098.3600	15.57	-19.58	-10.19
570	10	136.6323	136.5536	122.0181	34.2	34.1	30.5	16644.9900	-16608.1100	-13770.7700	15.91	-21.80	-10.72
570	0	97.2872	97.0791	81.8015	24.3	24.3	20.5	16182.1800	-29120.8500	-13407.6800	15.46	-23.86	-10.44
570	-10	58.6294	57.6294	42.9454	14.6	14.4	10.7	15050.0500	-30722.6000	-12383.7900	14.38	-25.17	-9.64
580	-20	18.6461	17.4561	3.1599	4.7	4.4	0.8	13989.1100	-32142.1900	-13592.1000	13.37	-26.34	-10.58

(II)

28V (mA)	TEMP	TEMP (COUNTS)			TEMP (°C)			BIAS (COUNTS)			BIAS (°/HR)		
		GX_	GY_	GZ_	GX_	GY_	GZ_	GX	GY	GZ	GX	GY	GZ
670	60	339.3872	342.7906	329.0858	84.8	85.7	82.3	10601.9600	-15152.1300	-857.3861	10.13	-14.48	-0.82
630	50	398.2064	300.5245	286.1069	74.6	75.1	71.5	12552.9400	-17161.6700	-8247.9910	11.99	-16.40	-7.88
600	40	256.8914	258.1629	243.9019	64.2	64.5	61.0	14752.4500	-18984.1700	-8561.6830	14.10	-18.14	-8.18
580	30	216.0421	217.0291	202.4237	54.0	54.3	50.6	16322.1900	-20907.0700	-9913.3700	15.60	-19.98	-9.47
570	20	176.7398	177.1590	162.6118	44.2	44.3	40.7	16339.500	-23336.9400	-10718.5600	15.61	-22.30	-10.24
570	10	136.7719	136.6614	122.0363	34.2	34.2	30.5	15964.5400	-26183.0600	-11278.8900	15.26	-25.02	-10.78
570	0	97.4546	97.2714	82.0232	24.4	24.3	20.5	15871.5200	-28977.5800	-12894.8600	15.17	-27.69	-12.32
570	-10	58.1021	57.4402	42.7710	14.5	14.4	10.7	15054.9500	-30508.2500	-12322.7500	14.39	-29.16	-11.77
580	-20	18.7004	17.6048	3.1549	4.7	4.4	0.8	14064.7200	-31981.6400	-13414.9500	13.44	-30.57	-12.82

(III)

Table 2. OTR results after compensation

28V (mA)	TEMP	BIAS(COUNTS)			BIAS(°/HR)		
		GX	GY	GZ	GX	GY	GZ
670	60	363.6606	261.3393	-1467.6890	0.35	0.21	-1.14
630	50	576.9733	-13.7218	2894.2040	0.55	-0.01	2.25
600	40	24.0543	88.8446	-308.9462	0.02	0.07	-0.24
580	30	280.9247	-79.4592	-1411.5110	0.27	-0.07	-1.10
580	20	-113.9939	-262.8186	-2234.0630	-0.11	-0.22	-1.74
570	10	-475.2744	330.9988	144.9579	-0.45	0.27	0.11
570	0	457.8644	-114.5547	-1031.9240	0.44	-0.09	-0.80
570	-10	522.0630	-34.6977	-2398.8360	0.50	-0.03	-1.87
580	-20	-669.9068	-1116.7990	-821.7973	-0.64	-0.92	-0.64

The overall bias values in terms of counts and $^{\circ}/\text{hr}$ for each temperature of a three axis gyro after compensation is shown in Table 2. The bias data of Gx varies from $(-0.11$ to $0.55)^{\circ}/\text{hr}$ & Gy bias data varies from $(-0.03$ to $0.21)^{\circ}/\text{hr}$ and Gz bias data varies from $(-0.24$ to $2.25)^{\circ}/\text{hr}$ which is effectively reduced as compared to before compensation. The bias drift varies approximately near to zero.

7. Conclusion

Thermal drift of three axis fibre optic gyroscope under different extreme temperatures are evaluated and compensated in this project. Temperature compensation in signal processing system using temperature soaking method is done which uses the linear curve fitting function to generate the bias error coefficients. The generated error coefficients are subtracted from the existing bias data, which in turn reduces the bias drift. The bias drift of each gyro is greatly reduced and it lies near to zero. This technique greatly improves the performance of gyro.

The main fact which restricts the use of the Soak method is required time, corresponding costs related to the equipment and manpower. Future work involves the use of advanced technique that may reduce the bias drift more efficiently to this method with less time.

8. References

- Nasiri-Avanaki MR, Soleimani V. Comparative assessment on the performance of open loop and closed-loop IFOGS. *Optic Photon J.* 2012; 2:17–29.
- Sternberg H. Qualification process for MEMS gyroscopes for the use in navigation systems. 2011 Oct.
- Juang J-N. Evaluation of ring laser and fibre optic gyroscope technology. 2012 Nov.
- Ghetia S, Gajjar R. Classification of fiber optical sensors. *International Journal of Electronics Communication and Computer Technology (IJECCT)*. 2013; 3(4):442–5.
- Karthik S. Under water vehicle for surveillance with navigation and swarm network communication. *Indian Journal of Science and Technology*. 2014 Oct; 7(S6):22–31.
- Udayakumar R, Khanaa V. Chromatic dispersion compensation in optical fiber communication system and its simulation. *Indian Journal of Science and Technology*. 2013 May; 6(6S):4762–6.
- Merlo S, Norgia M, Donati S. Fiber gyroscope principles. Italy: Electro Optics Group, University of Pavia; 2000.
- Gronau Y, Tur M. Digital signal processing for an open loop fiber optic gyroscope. *Applied Optics*. 1995 Sept; 34(25):5849–3.
- Khan MH. Open-loop fiber-optic gyroscope - a technical note. *Defence Science Journal*. 1996 Oct; 146(4):283–8.
- Bennett SM, Emge S, Dyott RB. Fiber optic gyroscope for vehicular use. *IEEE Jour Light Tach*. 1998; 1053–7.
- Sun QD, Zhu ZH, Larouche BP. FPGA-based hardware design of closed loop control for fiber optic gyroscope. *Journal of Theoretical and Applied Information Technology*. 2013 May 10; 51(1):121-8.
- Handrich E. Closed loop fiber optic gyro with shupe effect compensation. United States patent 20016181428 B. 2001.